



Contents lists available at ScienceDirect

Geotextiles and Geomembranes

journal homepage: www.elsevier.com/locate/geotexmem

Regular Paper

Effect of welding parameters on properties of HDPE geomembrane extrusion welds

R. Kerry Rowe^{a,*}, M. Mouhamed Ali^b^a Geotechnical and Geoenvironmental Engineering, GeoEngineering Centre at Queen's – RMC, Department of Civil Engineering, Queen's University, Kingston, K7L 3N6, Canada^b GeoEngineering Centre at Queen's – RMC, Department of Civil Engineering, Queen's University, Kingston, K7L 3N6, Canada

ARTICLE INFO

Keywords:

Geosynthetics
Extrusion welds
Fusion welds
stress cracking resistance (SCR)
HDPE
Geomembranes
Quality assurance

ABSTRACT

The stress crack resistance (SCR) of high-density polyethylene (HDPE) geomembrane extrusion welds is examined for a 1.5 mm HDPE geomembrane and three different welding parameter combinations (denoted as “Cool”, “Good”, and “Overheated”). Results are reported for unnotched welds, unnotched sheet, and notched sheet. The average SCR for a Good extrusion weld is 23% of that of the unnotched sheet SCR. Little variation is found between the three welding parameter combinations for low geometry irregularity SCR weld specimens. There is no statistically significant difference between a good-quality fusion and extrusion weld. However, operator-dependent weld induced geometric irregularity (WIGI) greatly affects the SCR of extrusion welds. Extrusion welds with high WIGI have an average unnotched SCR of only 9% of the unnotched sheet. Extrusion welds with an overground surface can have an unnotched SCR as little as 1% of the best extrusion weld. Deleterious weld bead geometries are identified to provide a framework with which engineers can identify “high-risk” extrusion welds with respect to stress cracking.

1. Introduction

High density polyethylene geomembranes (HDPE) are an essential component of the liner system used in many landfills and mining applications. These HDPE geomembranes are intended to contain fluids that could negatively impact the environment if they escaped, and it is important that they continue to contain the fluids for the entire contaminating lifespan of the facility (Rowe, 1988, 1991; Rowe et al., 2004). The time to nominal failure and service life of some HDPE geomembrane sheets may range from decades to millennia, depending on geomembrane material, temperature, chemical exposure, and the stress/strain in the field (Hsuan and Koerner 1998; Rowe et al., 2009; Tian et al., 2017, 2018; Morsy and Rowe 2020; Rowe et al., 2020; Morsy et al., 2021; Zafari et al. 2023a, 2023b, 2023c; Clinton and Rowe, 2023). One of the major factors affecting the service life of HDPE geomembranes is stress cracking when the geomembrane is exposed to sustained tensile loads or strains lower than the geomembrane's yield strength (Halse et al., 1990; Peggs and Carlson, 1990b; Seeger and Muller, 2003; Peggs et al., 2014; Francey and Rowe, 2022). Previous work suggested seven factors can induce stresses that can lead to brittle failure: gravel indentations, down drag on side slopes, differential

settlement, thermal contraction, geomembrane wrinkles, poor construction, and welds (Peggs and Carlson 1990a; Abdelaal et al., 2014; Ewais et al., 2014; Francey and Rowe 2022). Stress cracking associated with welds is often attributed to the quality of welds.

There are two common methods of welding HDPE geomembranes: fusion welding and extrusion welding. Most welds involve fusion welding of the edges of two geomembrane sheets (Scheirs 2009; Rowe and Shoaib 2017; Francey and Rowe 2022). Extrusion welding is normally used where fusion welding is not practical (e.g., for repairs, curves, and other welds not accessible to fusion welding machines (Seeger and Muller, 2003; Touze-Foltz et al., 2008; Scheirs 2009). Extrusion welding requires on-site preparation of the material (e.g., grinding) to be welded and requires a skilled operator capable of managing grinding depth/width, welding machine angle, welding speed, preheat and weld temperature, and the pressure on the welding bead (Toepfer 2015).

Most of the available studies on geomembranes are focused on investigating the short-term and long-term behaviour of geomembrane sheets (Seeger and Muller, 2003; Rowe and Islam 2009; Abdelaal et al., 2014; Ewais et al., 2014). Little research has addressed welding, and that research has focused on fusion welding and post-welding SCR short-term

* Corresponding author.

E-mail addresses: kerry.rowe@queensu.ca (R.K. Rowe), 18ma111@queensu.ca (M.M. Ali).<https://doi.org/10.1016/j.geotexmem.2023.12.002>

Received 11 September 2023; Received in revised form 8 December 2023; Accepted 12 December 2023

0266-1144/© 2023 Published by Elsevier Ltd.

behaviour (Zhang et al., 2017; Francey and Rowe 2022). To date, no studies have been performed to examine the effect of extrusion welding parameters on seam performance. This paper addresses this gap.

Welding locations are generally considered weak points in an HDPE geomembrane liner system (Peggs et al., 2014; Francey and Rowe 2022) and Rollin et al. (1999) reported that 55% of geomembrane failures in landfills, ponds, and basins were adjacent to welds. The predominance of failures at welds is often attributed to the quality of the welds. However, it is also known that geometry plays an important role for fusion welds, and it is not a far step to hypothesize that geometry will play a role for extrusion welds as discussed herein. As background, Giroud et al. (1995) showed theoretically that fusion welds act as a point of strain magnification due to bending stress induced by the eccentricity of the loading. Kavazanjian et al. (2017) performed experiments to measure the strain concentration resulting from welding and found that the maximum strain adjacent to the weld can range between 2.3 and 4 times the average specimen strain, with maximum strains reach to 1.4 to 2 times that estimated by theoretical model proposed by Giroud et al. (1995).

It has been suggested that stress cracks observed in the extrusion welded zones are due to excessive grinding and/or overheating (Halse et al., 1990; Peggs and Carlson 1990b; Hsuan 2000; Peggs et al., 2014). For instance, Hsuan (2000) examined rapid and slow crack failure at 16 different sites in three different countries (Canada, the United States of America, and Italy). The majority of failures were claimed to be associated with the extrusion weld and were occurring on the lower sheet adjacent to the weld, suggesting that material embrittlement occurred at this location due to over-grinding and/or over-heating. Emcon Associates (1994) inspected the Chiquita Canyon landfill liner after the 1994 Magnitude 6.7 Northridge earthquake. They reported that geomembrane tears were initiated at the extrusion welding bead or along the edge of the extrusion weld. Kavazanjian et al. (2013) performed a numerical analysis to investigate the causes of failure at the Chiquita Canyon landfill. It was concluded that earthquake induced failure of the geomembrane occurred at points of strain concentration and scratches.

It is commonly argued that the extrusion weld is an inferior type of welding in comparison to fusion welding (Darilek and Laine 2001; Toepfer 2015; Gilson-Beck and Giroud 2022), however there is limited evidence to support this claim. Gilson-Beck and Giroud (2022) investigated the leakage locations in 35 different projects obtained from electrical leak location survey (ELLS) survey results. The observed number of leaks associated with extrusion weld per unit length ranged from 60 to 100 times the number of leaks related to fusion weld per unit weld length. As such, it was concluded that, extrusion weld should be minimized as much as possible during the design and geomembrane installation. Peggs and Carlson (1990b) examined a limited number of extrusion and fusion weld specimens using the single point notch constant tensile load (SP-NCTL) for four different geomembranes. It was concluded that, SCR for extrusion and fusion welds examined was 56% and 46% of that of the sheet, respectively.

Francey and Rowe (2022) examined the effect of welding parameters on the unnotched SCR of un-aged fusion weld specimens for two sets of 1.5 mm thick HDPE geomembranes specimens over a range of welding parameters. They concluded that, for nine different welding parameter combinations, the average welding SCR value was 30% (ranges between 20% and 40%) of the unnotched sheet SCR; and the squeeze out geometry governs the SCR of the fusion weld. It was suggested to conduct SCR test on unnotched weld SCR specimens instead of notched SCR specimens as the unnotched welding SCR tests provide a more accurate estimate of SCR failure in the field. The unnotched welding SCR allows the failure to occur within the critical locations incorporating craze formation within the degraded region rather than occurring at the notch due to stress concentration.

Zhang et al. (2017) examined the effect of varying three welding parameters (i.e., low heat, standard, and high heat) on fusion welding's index properties such as Std-OIT, peel and shear strength/elongation,

and melt index. Zhang et al. (2017) found the area adjacent to the fusion weld, the heat affected zone (HAZ), had a small reduction in Std-OIT compared to the sheet. On the other hand, the squeeze-out bead of overheated fusion weld showed irregular thermograms and was suggested to be the result of sample inhomogeneity (i.e., non-uniform cooling, and non-uniform antioxidant consumption). To date, there have not been any published studies that examine the effect of extrusion welding parameter combinations on HDPE geomembrane welds. Thus, in view of the paucity of research investigating the unaged performance of the extrusion weld, the objective of this paper is to.

1. Evaluate the impact of welding temperatures on their Std-OIT, mechanical and physical behaviour.
2. Examine the effects of weld-induced geometric irregularity (WIGI) on SCR of extrusion welds.
3. Examine the effect of over-grind and defects adjacent to the extrusion welds on SCR.
4. Compare SCR performance of unnotched HDPE geomembrane extrusion and fusion welds.

2. Material and methods

2.1. Geomembrane examined

Extrusion welding of a 1.5 mm HDPE flat die geomembrane (denoted MwA-15) was examined (Table 1). MwA-15 was manufactured in 2011 with an virgin Std-OIT_o of 162 ± 4min, HP-OIT_o of 1320 ± 12min. and SCR_o (ASTM D5397 (ASTM 2020)) of 1080 ± 83 h with all exceeding the requirement of GRI-GM13 (2019). The geomembrane sheets had been stored in the laboratory fridge for 8 years before welding was applied to the sheets to avoid oxidation depletion or stress relaxation of the sheet.

2.2. Welding Procedure

The geomembrane surfaces were prepared by cleaning and grinding to remove the oxidized surface and waxy layers (Hsuan, 2000; Scheirs, 2009; Toepfer, 2015; Gilson-Beck and Giroud, 2022). The extrusion welding was performed by a licensed geosynthetic installer using a Demtech extruder at a landfill site on a summer day when the geomembrane sheet temperature at the time of the welding was 37 °C. In

Table 1
Index properties for examined geomembrane, MwA-15.

Properties	Method	Unit	GMB1
Nominal thickness	ASTM D 5199	Mm	1.5
GMB designation			MwA-15
Manufacturing date			2011
Manufacturing technique			Flat die
Standard oxidative induction time (Std-OIT)	ASTM D 3895	Min	165 ± 2
High-pressure oxidative induction time (HP-OIT)	ASTM D 5885	Min	1321 ± 12
Suspected HALS			Yes
HLMI (21.6 kg/190 °C)	ASTM D 1238	g/10 min	19.5 ± 0.5
SCR _o	ASTM D 5397	Hours	1012 ± 85
SCR _m	ASTM D 5397	Hours	616 ± 85
Yield stress for SCR		kN/m	29.3
Tensile yield strength (MD)	ASTM D 6693	kN/m	29.6 ± 0.5
Tensile yield strain (MD)	Type (IV)	%	19.7 ± 0.3
Tensile break strength (MD)		kN/m	46.4 ± 0.3
Tensile break strain (MD)		%	760 ± 13.8

each case, the geomembrane sheets were preheated (to temperature T_p) with hot air to reduce the amount of heat required and increase the size of the molten bead (extrudate) and avoid thermal shock that can lead to weakening of the polymeric structure along the edge of the welding bead (Mollard et al., 1996). The welding rod, made from the same resin as the sheet, was melted in the barrel of the extruder (to temperature T_e) and then extruded under a pressure dictated by the welder to bind the top and bottom geomembranes surfaces together (Fig. 1). The weld was allowed to cool naturally in the sun before being transported to the laboratory and stored at 21 °C. According to DVS 2225-1 (2016), in the field, the typical preheat temperature used ranges from 230 °C to 300 °C, and the barrel temperature used ranges from 190 °C to 240 °C. As the extrusion weld is a manual welding technique, the welding speed (which ranges from 0.2 to 1.2 m/min; DVS 2225-1, 2016) and pressure mainly depend on the operator.

Adopting the general approach described above, three welding scenarios were examined (denoted “Overheated”, “Good”, and “Cool”, Table 2). The high heat (“Overheated”) cases had a preheat temperature $T_p = 277$ °C and barrel temperature $T_e = 288$ °C. The “Good” weld cases had $T_p = 220$ °C and $T_e = 230$ °C. Finally, “Cool” welding cases had $T_p = 150$ °C and $T_e = 230$ °C (Table 2).

The extruder had a temperature gauge indicator at the nozzle, allowing adjustment of preheat and barrel temperatures (T_p , T_e). However, the welding speed and pressure depend primarily on the operator’s skills. An operator inducing high pressure will generate a Welding Induced Geometric Irregularity (WIGI) (Fig. 2).

2.3. Standard oxidative induction time

STD-OIT tests were conducted in a similar setting to that of (ASTM D3895 (ASTM 2019)) using a TA instruments Q-2000 series differential scanning calorimeter (DSC). STD-OIT tests were used to assess the quantity of antioxidants present in the geomembrane sheet and evaluate the effect of extrusion welding parameters on the oxidation resistance of the welding area by testing the quantity of antioxidants retained in the Std-OIT extrusion welding specimens at eight locations (Fig. 3) on the post-welded specimens.

2.4. Melt flow index

The melt flow index (MFI) tests (ASTM D1238 (ASTM 2013)) were performed to infer the change in molecular weight of the polymer, which is related to cross-linking and/or chain-scission degradation (Hsuan and Koerner 1998). MFI has also been examined for extrusion welds to assess the material compatibility of extrudate bead (Scheirs 2009).

2.5. Stress crack resistance testing

Stress crack resistance testing (SCR) was conducted on notched (ASTM 2020, GRI-GM5(c)), unnotched sheet and unnotched welds. SCR tests were performed on unnotched welds by positioning the heat-affected zone adjacent to the flashing area in the centre parallel region. SCR testing was conducted by immersing standardized 60 mm

long by 12.7 mm wide SCR dumbbell specimens (Fig. 4) in a 10% IGE-PAL solution at 50 °C elevated temperature and subjected to an applied load equal to 30% of the yield stress.

Rowe and Shoaib (2018) found that the material directly adjacent to the fusion weld (i.e., heat-affected zone, HAZ) aged more rapidly than the sheet. The HAZ is, therefore, a weak point and potentially where brittle failure starts (Halse et al., 1990; Peggs and Carlson, 1990a; Peggs et al., 2014; Marta and Armstrong, 2020; Francey and Rowe, 2022). Thus, the critical zone (CRIT) is identified in this study as the point located at the junction of the lower geomembrane sheet and the flashing at the end of the weld (Fig. 4).

Francey and Rowe (2022) recommended the use of unnotched SCR testing of welds as a more reliable testing metric for examining the SCR of HDPE welds because it better simulates field loading conditions than the notched test. This is due to the unnotched welding specimens allowing the welding specimen to initiate cracking in the critical location, similar to what would occur in the field (Francey and Rowe, 2022). Additionally, this method allows the specimen to initiate a crack and then propagate through the specimen from the point of weakness rather than a prescribed initiation point defined by the notch. Typically, in an unnotched specimen, a stress crack originated at CRIT and extended perpendicular to the applied load direction toward the opposite sheet side with the brittle detachment zone as shown in Fig. 5. The corresponding failure time incorporates the time for craze formation and crack propagation (Francey and Rowe, 2022).

3. RESULTS and discussion

3.1. Standard oxidative induction time (Std-OIT)

Std-OIT tests were examined, for three different welding parameter combinations, the sheet material and welding material rod. Std-OIT test specimens were taken from different locations along the welding cross-section, including welding bead, HAZ, and flashing (Fig. 3) from each type of welding.

Location 1 (Fig. 3) was the unaged geomembrane sheet away from the weld (SAW), which was unaffected by the welding. Locations 2 and 8 (the heat-affected zone, HAZ1) were located at the edge of the flashing adjacent to the weld track. Locations 4 and 6 (the heat-affected zone, HAZ2) were sampled from the sheet between the flashing and the weld bead. Location 5 was on the weld bead, and locations 7 and 8 were located at the flashing (squeeze-out) produced during the extrusion weld. The Std-OIT tests were performed on three replicates of each location (i.e., three specimens were examined from each location, totalling 24 specimens). The average initial STD-OIT and standard deviations of the examined locations are shown in Table 3.

The welding rod was heated and melted in the barrel of the extruder to create the extrudate bead. The welding rod material had an average initial STD-OIT₀ of 348 min (essentially twice that of the geomembrane away from the weld). The measured Std-OIT at the welding bead and flashing was less than that of the welding rod material but substantially more than the sheet material. The heat-affected zone (HAZ), located adjacent to the flashing, was not melted during the welding but was heated with a temperature sufficient to affect the microstructure and

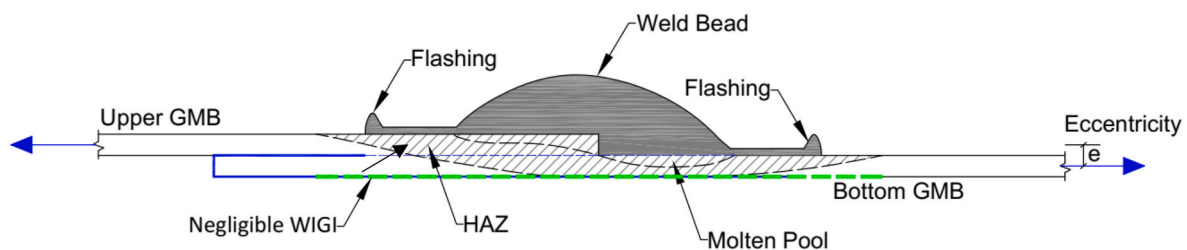


Fig. 1a. Schematic cross-p of a typical extrusion welded.

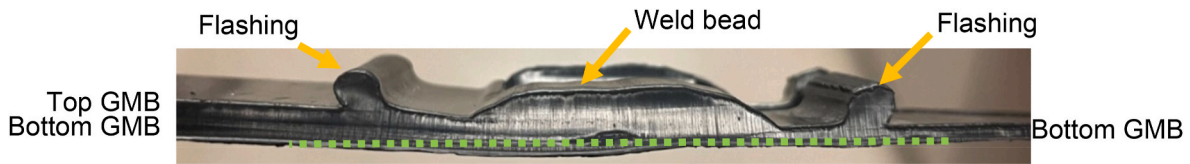


Fig. 1b. Photographic cross-section view of HDPE extrusion weld.

Table 2

Matrix of extrusion welding parameters to be examined (T = temperature).

Parameter Combination	1	2	3
Sheet T (°C)	37	37	37
Pre-heat T (°C)	150	220	277
Barrel T (°C)	230	230	288
Weld Description	Cool	Good	Overheated
Grinding	Normal	Normal	Over
GMB	MwA-15		

may increase the crystallinity (Sieracke and Peggs, 2013). Flashing zone locations 3 and 7 had reduced to 50% of the rod's initial value but were still higher than that of the sheet at the Cool and Good welding. The average Std-OIT values at locations 2 and 4 (heat-affected zones) showed no statistically significant difference from the sheet away from the weld for any of the welding parameter combinations examined (Table 3). This suggests that, in this specific case, the extrusion welding had a negligible effect on antioxidant oxidation (AO) resistance of the heat-affected zone for the geomembrane and welding conditions examined. The initial Std-OIT of flashing (locations 3 and 7) for Cool, Good, and Overheated welding parameters was 9%, 11%, and 65% greater than that of the sheet, respectively (Table 3). The Std-OIT of the welding bead (location 5) for Cool, Good, and Overheated weld were about 50% of that of the rod but 4%, 12%, and 7% above that of the

sheet (SAW), respectively (Table 3).

Although the welding rod and the geomembrane are made of the same resin, the Std-OIT of the rod was double relative to the sheet. This raises the question: in geomembrane applications, should the welding rod be required to have twice the OIT of the geomembrane to ensure the quality of the welds, even if they are made from the same resin? After welding, the bead zone had similar or slightly more Std-OIT than the sheet and hence, in terms of initial post-welding conditions, the weld had not compromised the integrity of the liner from the perspective of the antioxidants. The post-welding Std-OIT values for all examined welding parameters were higher than that required for a new geomembrane meeting the requirements of GRI-GM13 (2019).

3.2. Melt flow index (MFI)

The MFI was performed to assess the compatibility of the HDPE geomembrane after welding. The welding rod was mixed with the geomembrane sheet material to form the bead zone. MFI for welding rod material and geomembrane sheet were 15.7 and 22, respectively. The extrudate bead had the same melt index as the rod material (Fig. 6), indicating compatibility between the welding rod and the sheet.

3.3. SCR performance

Notched sheet, unnotched sheet and unnotched weld specimens were

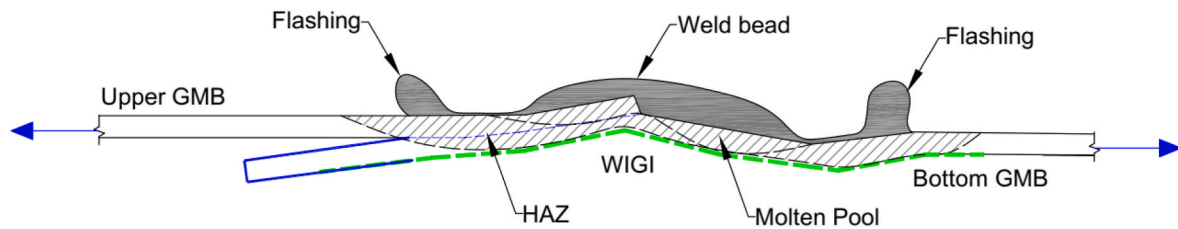


Fig. 2a. Schematic cross-section of a typical extrusion welded. (Welding induced geometric irregularity, WIGI).



Fig. 2b. Photographic cross-section view of HDPE extrusion weld. (Welding induced geometric irregularity, WIGI).



Fig. 3. Photo of the extrusion weld cross-section, which shows locations of the sampling for the Std-OIT test and crystallinity test.

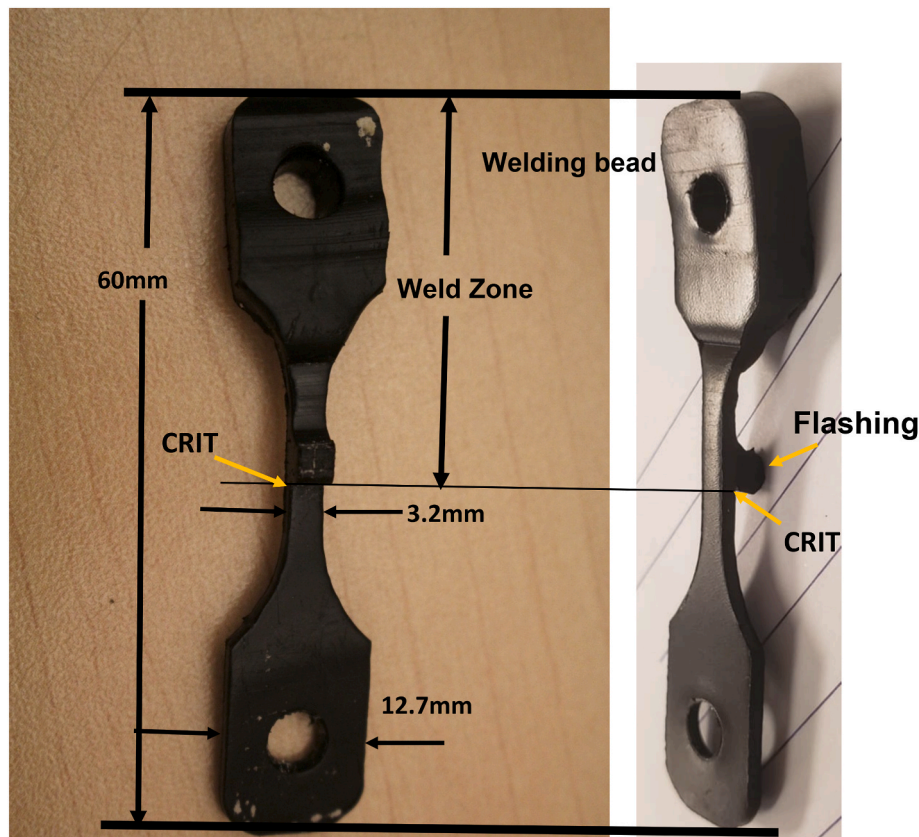


Fig. 4. SCR standard extrusion weld specimen and position of HAZ. The critical zone (CRIT) for stress cracking initiations occurs at the HAZ adjacent to the flashing area (end of welding area).

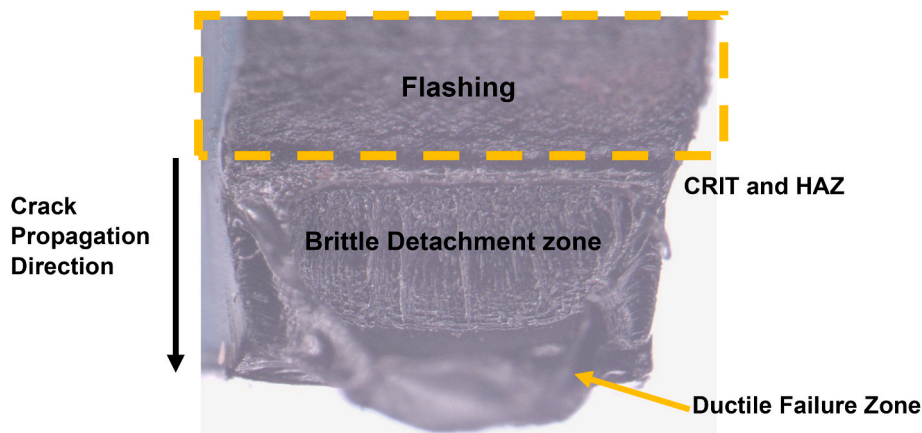


Fig. 5. Unnotched extrusion weld failed specimen to capture the effect of the welding and show potentially degraded material within the brittle detachment zone of an SCR specimen.

subjected to a constant tensile load equal to 30% of the yield strength for their corresponding cross-sectional area. The average unnotched MwA-15 SCR weld failure times (Table 4) for the three welding parameter combinations (i.e. Cool, Good, and Overheated) was 2674 ± 1068 h. The average unnotched MwA-15 sheet failure times were 11740 ± 3320 h. The notched MwA-15 sheet failure time averaged 1012 ± 85 h. The ratio of the unnotched weld SCR to the unnotched sheet was 0.23 ± 0.1 , indicating a 4.4-fold drop in unnotched SCR due to the welding. This corresponds very closely to the average ratio of 0.25 ± 0.1 for unnotched MwA15 fusion weld SCR to unnotched geomembrane sheet SCR reported by Francey and Rowe (2022) after normalized to average unnotched sheet SCR of 11740 h.

There was no statistically significant difference between the mean SCR of the three extrusion weld categories (viz: 2473 ± 1625 , 2889 ± 1379 and 2520 ± 1767 h; Table 4) examined, suggesting that changes in preheated and barrel temperatures at the welding time had a limited effect on welding SCR for the geomembrane and range of welding parameter examined. However, there was substantial variation in each category and particularly low values (1324 h for a Cool weld and 1061 h for an Overheated weld). This suggests that another factor may control the shorter SCR failure time for the extrusion welded specimens. The variation between welded SCR specimens was hypothesized to be due to the differences in geometry of the welded specimens, which affects the strain/stress at the critical location, CRIT (e.g., Fig. 7).

Table 3
STD-OIT values of the sheet and post-weld extrusion weld zone.

Welding Temperatures	HAZ1 ^a "2&8"	Flashing zone "3&7"	HAZ2 "4&6"	Bead zone "5"	SAW ^b	Rod
150 °C/230 °C	156 ± 4	176 ± 2	166 ± 11	168 ± 8	162 ± 4	348 ± 16
220 °C/230 °C	159 ± 3	179 ± 3	157 ± 1	181 ± 1		
277 °C/288 °C	156 ± 1	268 ± 111	178 ± 33	173 ± 1		

^a Heat affected zone.

^b Geomembrane sheet away from welding.

3.4. Quantification of the extrusion weld irregularity

With fusion welds, the quality is dependent on appropriate machine settings, but once they are in place, highly consistent welds can be obtained due to the automated nature of the welding process. With extrusion welds, the pre-heat and barrel temperatures need to be appropriately set for the current sheet temperature and ambient weather conditions. As indicated in the previous section, although these machine

settings are important, they are not the only variable controlling the consistency and quality of extrusion welds because of this welding technique's dependence on the skills and experience of the welder. Thus, an appropriate combination of heat, speed, and pressure is required to obtain a consistent high-quality extrusion weld with high stress crack resistance. In contrast, a low-quality extrusion weld may lead to welding-induced geometric irregularity (WIGI) on the bottom surface of the welding zone. This irregularity to the consistency and appropriateness of the applied pressure exerted manually by the operator. Due to this dependence on human consistency with respect to the speed and applied pressure during welding, minimizing the risk of premature stress cracking of extrusion welds necessarily requires very good construction quality control and quality assurance (Hsuan, 2000). The welding irregularity (WIGI) can lead to low stress crack resistance (SCR) due to stress/strain concentration adjacent to the flashing (point a; Fig. 7) and between the flashing and bead zones (point b; Fig. 7). In cross-section, WIGI can be recognized visually by looking at the bottom surface of the geomembrane extrusion weld (e.g., compare bottom surface Fig. 1b and 2b). When viewing only from the surface, WIGI available is more difficult to identify, but nevertheless can be identified in many cases by the surface expression (e.g., compare top surface Fig. 1b and 2b). The

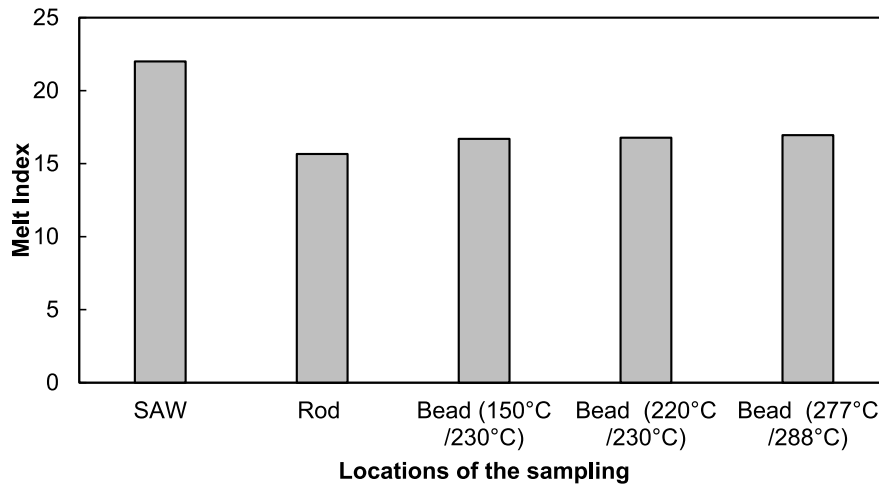


Fig. 6. Melt flow index (21.6 kg) results for bead extrusion weld, welding rod material and unaged SAW.

Table 4
MwA-15 SCR Failure times for unnotched weld specimens. Welded samples normalized to unnotched sheet equivalent.

Material	Type	Notch	Sheet temperature at the time of welding (°C)	Preheat Temp (°C)	Barrel Temp (°C)	Average Failure Time (hours)	STD. Dev	Normalized average failure time ^a	Maximum (hours)	Minimum (hours)	
MwA-15	virgin sheet	Notched	37	N/A	N/A	1012	85		1097	896	
	virgin sheet	Unnotched		N/A	N/A	11740	3320	1	16963	8275	
	Weld				150	230	2473	1625	0.21	3622	1324
					220	230	2889	1379	0.25	3384	2201
					277	288	2520	1767	0.21	4484	1061

^a Normalized to unnotched sheet equivalent.

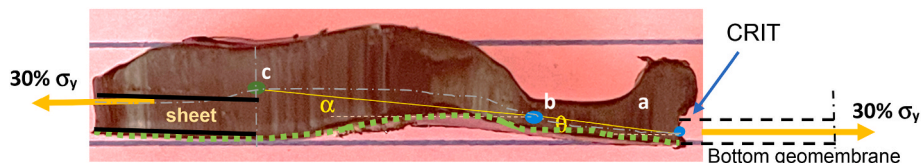


Fig. 7a. Photographic cross-section view of a typical high geometry irregularity (WIGI) extrusion weld specimen after failure in stress crack test.

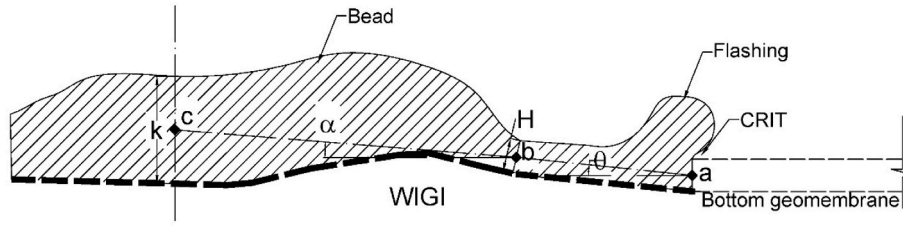


Fig. 7b. Cross-section view of a typical high geometry irregularity (WIGI) extrusion weld specimen after failure in stress crack test.

WIGI index quantifies the geometric irregularity in terms of the rotation of the upper sheet, extruded bead, and bottom sheet relative to the combined thickness of the bead and geomembrane located between flashing and bead zones (Fig. 7). The WIGI index, μ , can be written as follows.

$$\mu = (\theta + \alpha) H/k \quad (1)$$

and WIGI, ω , is given by

$$\omega = \mu - \mu_0 \quad (2)$$

as defined with respect to Fig. 7:

Point "a" is located at the centerline of the bottom geomembrane at CRIT;

Point "b" is located at the centerline of welded geomembrane at starting of the bead zone;

Point "c" is located at the centerline of the bead at the loading position.

H = HAZ thickness at point "b";

k = Bead thickness at point "c";

θ = angle between the horizontal line and the line between points a and b in radians;

α = angle between the horizontal line and the line between points b and c in radians

μ_0 = WIGI index at low welding irregularity = 0.032;

The normalized SCR (λ) and WIGI (ω) values for the virgin extrusion welds were plotted in Fig. 8.

$$\lambda = SCR/SCR_{w0} \quad (3)$$

where SCR_{w0} is the stress crack resistance at low WIGI (in this case $SCR_{w0} = 6100$ h (i.e., at $\mu \sim 0.032$, $\omega \sim 0$; Fig. 8).

SCR tests were conducted using dogbone weld specimens that were carefully prepared to avoid changing WIGI. These welds and unnotched sheet specimens were then subjected to a constant tensile stress equal

30% of the unnotched yield stress of the sheet material. As this stress is transferred from the sheet on one side of the weld to the sheet on the other side of the weld, an eccentricity between the two sheets leads to an increase in stress/strain concentration (Fig. 7) even for a good weld with low WIGI ($\mu \sim 0.032$, $\omega \sim 0$) the highest SCR, $SCR_{w0} = 6100$ h (i.e., 52% of the unnotched sheet value of 11,740 h). The eccentricity increases with increasing WIGI and consequently increasing ω . Although excess pressure during welding can cause an increase in WIGI at any temperature, it tended to occur more often with Cool and Overheated welding parameters. In the case of Cool welds, more pressure was required to get a quality extrusion weld and an overestimate of that applied pressure was more common with the more difficult Cool polymer. Conversely, in the Overheated case, less pressure was required and it was even easier to misjudge the pressure and obtain high WIGI.

For welds with a thick extrudate bead, the extraction of the SCR specimen from the cutting die can be challenging. The use of cyclic loading (e.g., hammering) or high pressure to extract the dogbone specimen from the die may lead to a reduction in the failure time that can reach 250 h for Good welding parameters combinations. Therefore, more care during the extraction and preparation of the specimens is required to avoid SCR reduction due to human errors.

Fig. 8 shows the relationship between the normalized SCR in terms of λ and ω in terms of the difference in WIGI between a particular weld and a weld with minimal WIGI. The dashed line represents an empirical relationship between λ and ω based on virgin examined weld specimens as follows:

$$\lambda = -0.182 \ln(|\omega|) - 0.5557 \quad (4)$$

The virgin extrusion weld with the highest $SCR_{w0} = 6100$ h had $\omega = 0$ ($\mu = 0.032$). The SCR rapidly decreased to 1320 h rapidly with an increase in $|\omega|$ to 0.013 ($\mu = 0.045$; Table 5 (virgin specimens)).

To this point, the discussion of SCR has been restricted to virgin specimens.

3.4.1. Validate the proposed WIGI quantification approach using early-aged extrusion welds

To assess the effectiveness of the proposed WIGI quantification approach on aged geomembranes, additional samples immersed in simulated municipal solid waste (MSW) leachate at 85 °C were periodically sampled, and these gave $SCR_{predicted}$ and SCR_{actual} values consistent with those for the virgin specimens at relatively early stages of the ageing process (Fig. 9). With continued ageing, the $SCR_{predicted}$ failure times from Eq. (4) experienced relatively little change as shown for a number of cases in Fig. 10. It is very difficult to get two or more extrusion welds with exactly the same WIGI. However, in a number of cases, fairly comparable WIGI values were obtained for specimens from the same WIGI aged for different lengths of time, and hence aged values had $SCR_{predicted}$ from Eq. (4) that followed a path shown by arrows in Fig. 10 showing a fairly consistent $SCR_{predicted}$ with a decrease in SCR_{actual} with time to a little over 1000 h which appears to be the representative value for the material and was somewhat less dependent on WIGI values for $|\omega| < 0.008$. For $|\omega| > 0.008$, the initial SCR_{actual} was less than 2000 h and aged specimens with high ω failed at very low SCR. A plot of SCR for different values of WIGI, μ , for both aged and virgin

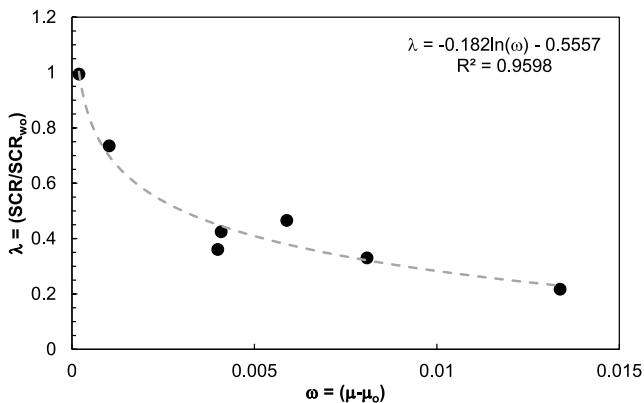


Fig. 8. Variation of unaged extrusion weld geomembrane normalized SCR (λ) versus ω (Note: the dashed line is the theoretical line based on Eq. (4)).

Table 5
Values of WIGI index (μ), ω , and measured SCR for the examined extrusion weld specimens.

Incubation time (months)	θ (Degree)	α (Degree)	$\theta + \alpha$ (Degree)	Bead/HAZ2	μ	$\omega = \mu - \mu_0$	SCR _{actual} (hours)
virgin	2.2	6.7	8.9	4.1	0.0379	0.00589	2841
	1.2	7.1	8.3	4.5	0.0322	0.00019	6066
	5.9	6.3	12.2	5.9	0.0361	0.00409	2590
	3.4	6.5	9.9	4.8	0.0360	0.00400	2201
	5.3	5.1	10.4	4	0.0454	0.01338	1324
	0	7	7	3.7	0.0330	0.00102	4484
3m	6	4.68	10.68	4.65	0.0401	0.00809	2015
	6.3	8.9	15.2	4.6	0.0577	0.02567	293
	7.6	3.2	10.8	3.8	0.0496	0.01760	820
6m	0	9.1	9.1	4.2	0.0378	0.00582	2100
	0	4.8	4.8	3.8	0.0220	0.00995	2134
7.9	0	15.47	15.47	3.7	0.0730	0.04097	912
	6.1	4.9	11	3.5	0.0549	0.02285	885
9	-2.5	5.1	2.6	3.8	0.0119	0.02006	995
	-3	5.3	2.3	4.4	0.0091	0.02288	1294
15	1.6	13.2	14.8	3.9	0.0662	0.03423	1406
	0	6.7	6.7	4.8	0.0244	0.00764	2279
	13	-1.8	11.2	3.9	0.0501	0.01812	1086
19	0	7.8	7.8	4	0.0340	0.00203	1535
	0	6.3	6.3	4.3	0.0256	0.00643	1535
	-1.7	5.6	3.9	5.6	0.0122	0.01985	1904
22	7.4	3.57	10.97	3.4	0.0563	0.02431	1378
	2	15.1	17.1	3.7	0.0807	0.04866	1173
	10.4	-3.6	6.8	3.4	0.0349	0.00291	1235
24	2.4	0.5	2.9	4.5	0.0112	0.02075	2352
	3.34	1.1	4.44	3.3	0.0235	0.00852	1217
	3.64	14.76	18.4	3.9	0.0823	0.05034	885
24	0.54	8.7	9.24	4	0.0403	0.00832	2390
	9.3	-3.1	6.2	3.5	0.0309	0.00108	1361
	-2	-1.15	-3.15	4.6	-0.0120	0.04395	1550
	4.16	9.62	13.78	4.34	0.0554	0.02341	146

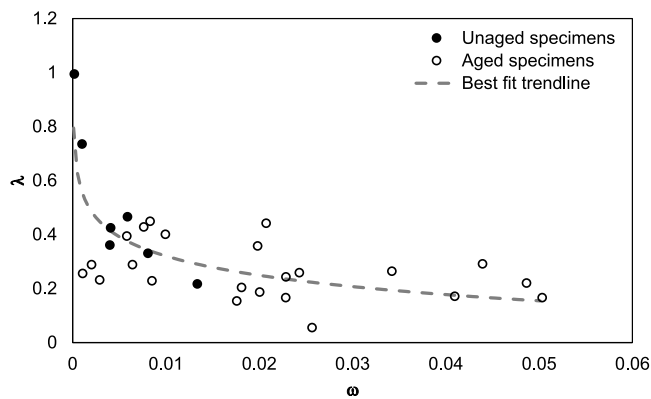


Fig. 9. Variation of λ versus ω for unaged and aged extrusion welds geomembrane specimens.

specimens (Fig. 11 and Table 5) identifies the high-risk zones as the situations where $|\omega| > 0.008$ ($\mu < 0.02$ or $\mu > 0.04$) and welds with WIGI $|\omega| > 0.008$ should be considered to have a high-risk of a low SCR.

While identifying high-risk areas can be beneficial for construction quality assurance, the presented approach may seem complex to implement. Therefore, users can simplify obtaining WIGI by following these steps. First, assess the magnitude of WIGI using cut destructive testing specimens after welding. Then, capture a picture of the cross-section of these welded specimens and use AutoCAD to measure the rotation angles at points a and b (Fig. 7) and the relative thickness of H and K. Next, apply equation (1). If welding irregularities on the bottom surface with a high ω are observed, less pressure is required, and appropriate changes to the welding parameter combinations can be made to limit the degree of WIGI.

The current study demonstrates that equation (1) can be used to assess the effect of WIGI on the SCR of the extrusion welds, and equation

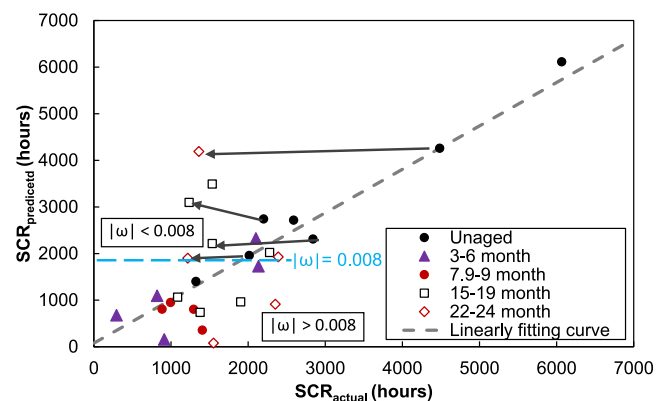


Fig. 10. Comparison between measured SCR failure time versus predicted SCR failure time of examined extrusion weld Geomembranes specimen unaged and aged specimens in different incubation time stages at 85 °C immersed in MSW-L3.

(4) can predict the reduction in the SCR due to WIGI magnitude. However, this study only examined one 1.5 mm smooth geomembrane (virgin and early-aged specimens) and did not investigate the SCR reduction due to WIGI for different geomembrane thicknesses or very aged specimens. This requires further research.

3.5. Overgrind effect

HDPE geomembranes have low molecular weight chains, so-called oligomers, that can bloom and create a waxy layer that restricts welding and causes adherence difficulty. To remove the oxidized surface, dirt, dust and additive blooms, the areas of the geomembrane to be extrusion welded generally need to be ground before welding (Scheirs, 2009; Toepfer, 2015; Gilson-Beck and Giroud, 2022). However,

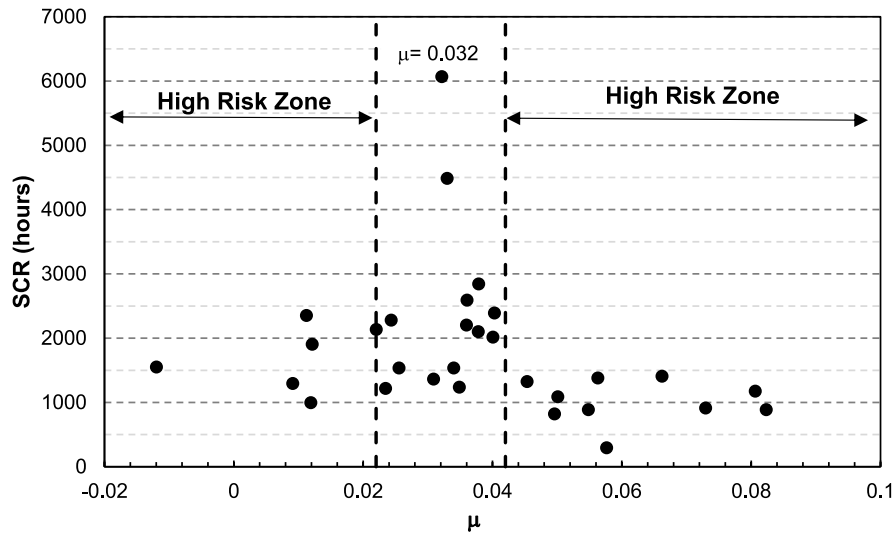


Fig. 11. Variation in SCR failure time for aged and unaged versus WIGI index “ μ ”. The dashed line is the transition between high-risk zones of WIGI and normal WIGI.

improper grinding (e.g., when the overground extends beyond the area to be welded) has been reported to cause a reduction in the geomembrane thickness adjacent to the weld area, leading to an increase in the stress/strain concentration (Giroud et al., 1995; Giroud, 2005). The poor geomembrane surface preparation can leave contaminated waxy layers, leading to poor in-plane welding integrity (Scheirs, 2009; Gilson-Beck and Giroud, 2022). The ideal grinding should equal to a depth of 4% of the HDPE geomembrane thickness and should not exceed 10% of the geomembrane thickness, while the ground width should not exceed the extrudate bead width (Scheirs, 2009; Toepfer, 2015).

The overground extrusion welds examined in this study had a reduction in the sheet thickness adjacent to the flashing ranging between 16 and 33% of geomembrane sheet thickness due to over-grinding (Fig. 12). The strain concentrations increase due to the improbable grinding (Giroud et al., 1995). The strain concentration is an indicator of stress cracking, and stress cracks could result from excessive over-grind (Hsuan, 2000).

For all the weld specimens examined, failure occurred again as a

brittle failure and this continued until the thickness was reduced sufficiently for the stress over the remaining area to increase the point that the failure continues in a ductile manner (e.g., Figs. 13 and 14). All virgin overground extrusion weld specimens exhibited brittle failure surfaces progressing to plastic failure. The average SCR for overground welds examined (two Good and three Overheated specimens) was 168 ± 69 h (Fig. 15). The SCR for overground specimens decreased by 98% compared to the unnotched sheet SCR (Fig. 15). The point of maximum thickness reduction due to overground in the bottom geomembrane served as the point of crack initiation at failure and gave failure surfaces, as shown in Figs. 13 and 14. This suggests that increased stresses within the overground surface aid in craze formation through embrittlement. Furthermore, the reduction in the bottom geomembrane thickness reduces failure time due to the decrease in the effective cross-sectional area of the SCR specimen, leading to an increase in the local stresses along the overground zone.

The combination of overground and high WIGI increases the strain concentration at the weld and decreases the stress crack failure time.

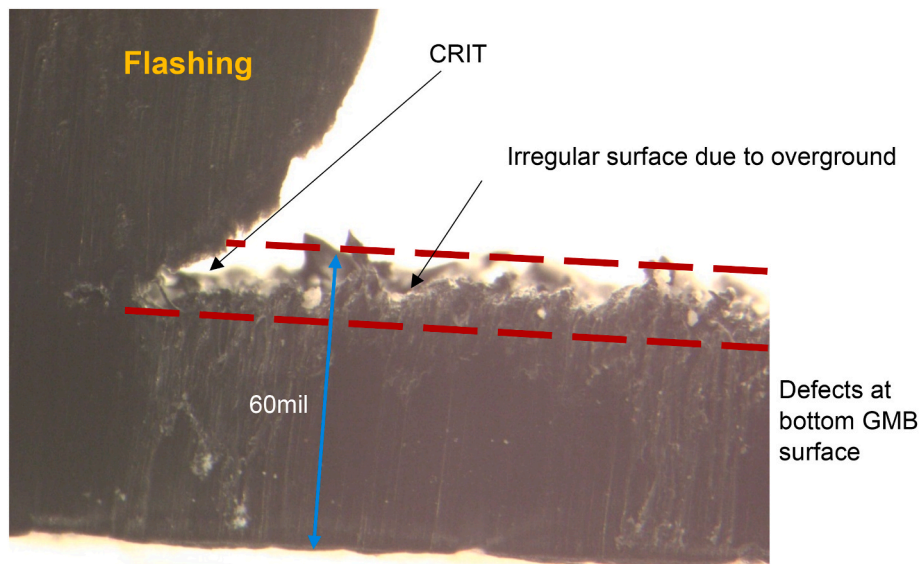


Fig. 12. Unaged over ground welded Geomembrane specimen adjacent to the flashing (photo under a microscope).

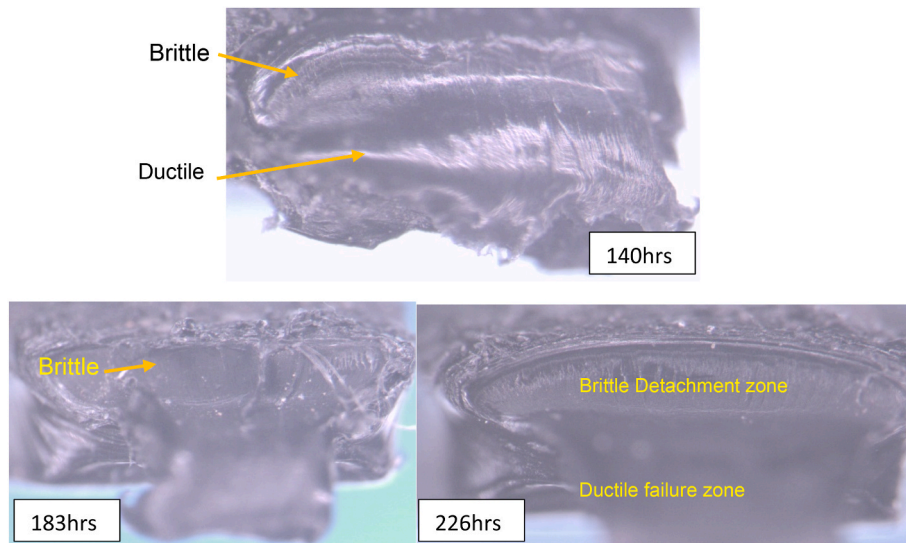


Fig. 13. Unnotched overhead extrusion weld failed specimen to capture the effect of the overground.

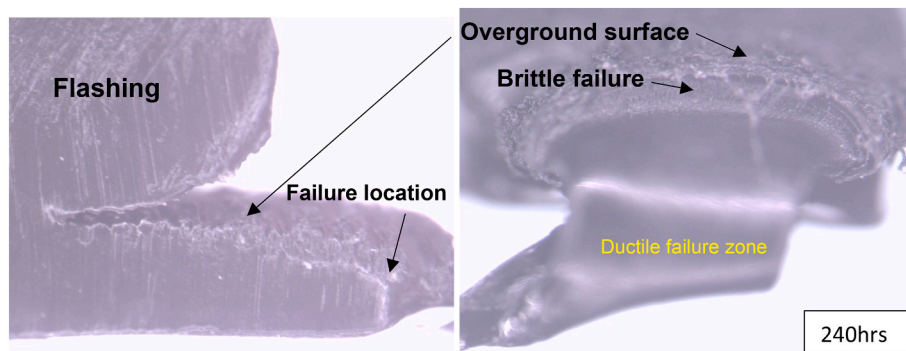


Fig. 14. Stress cracking was found in the Geomembrane sheet away from CRIT due to Geomembrane thickness reduction occurring due to excessive over-grinding of the sheet.

Therefore, inspecting the overground regions should be considered during the destructive tests. In addition, the visual inspection of the extrusion weld integrity gives insights into critical locations (i.e., grinding beyond the welding bead, high WIGI, and scratches at CRIT).

Scratches on the geomembrane surface and defects at CRIT (Fig. 16a) were found to be locations increased the strain concentration due to the reduction of the thickness. As the interface between HAZ1 and melt solidified, interface between the two may act as a notch to initiate stress crack (Sieracke and Peggs, 2013). The craze of unnotched virgin extrusion weld geomembrane can initiate as an angle (Fig. 16).

3.6. Comparison of virgin extrusion with fusion weld performance for MwA-15

Virgin unnotched SCR of extrusion welds examined in this study are compared with virgin SCR of fusion welds examined by Francey and Rowe (2022) in Table 6. Unnotched SCR test specimens' failure surfaces for extrusion welding exhibited brittle detachment and ductile detachment regions, similar to the fusion weld examined by (Francey and Rowe 2022). The average unnotched SCR failure times for six-fusion weld parameter combinations was 2700 ± 760 h (coefficient of variation, COV = 28%; Table 6). The average unnotched SCR failure times for the three-extrusion welds parameter combination were 2630 ± 1285 h (COV = 49%; Table 6).

Thus, there is no statistically significant difference (at the 95% confidence level) between the average SCR for a fusion and normal Good

extrusion welds. Thus, extrusion welds are not necessarily bad; but, they are more susceptibility to operator-induced variability and are more likely to be problematic such that low-level quality control, allowing overground, and/or high WIGI welds to pass, will result in lower SCR than fusion welding. However, this raises the question of whether the long-term performance of extrusion and fusion welds would be similar, especially for the overheated (for both welds) and high WIGI specimens. Further investigation is required to answer the question and examine the effect of seam longevity.

The greatest cause of low SCR for extrusion welded specimens was overheating of the polymer melt during welding and/or geometry of weld, with the lowest SCR being manifest for welds with high WIGI and/or grinding surface extending beyond the welding bead. The greatest cause for low SCR of fusion welds was a combination of a high wedge temperature of 460°C and a low wedge speed of 1.8 m/min (Francey and Rowe, 2022) for sheet temperatures of 65°C and 21°C . Extrusion welds exhibiting overground for Good and Overheated welding parameters could result in thickness reductions as much as 0.5 mm and resulted in the greatest observed reduction in welding SCR failure time (minimum value 3% of the average weld failure time and 10% of the notched sheet SCR).

3.7. Practical implications construction quality control and assurance

The extrusion weld examined with Good temperature and low WIGI ($0.022 < \mu < 0.042$, see Fig. 1) had a similar unnotched SCR as the fusion

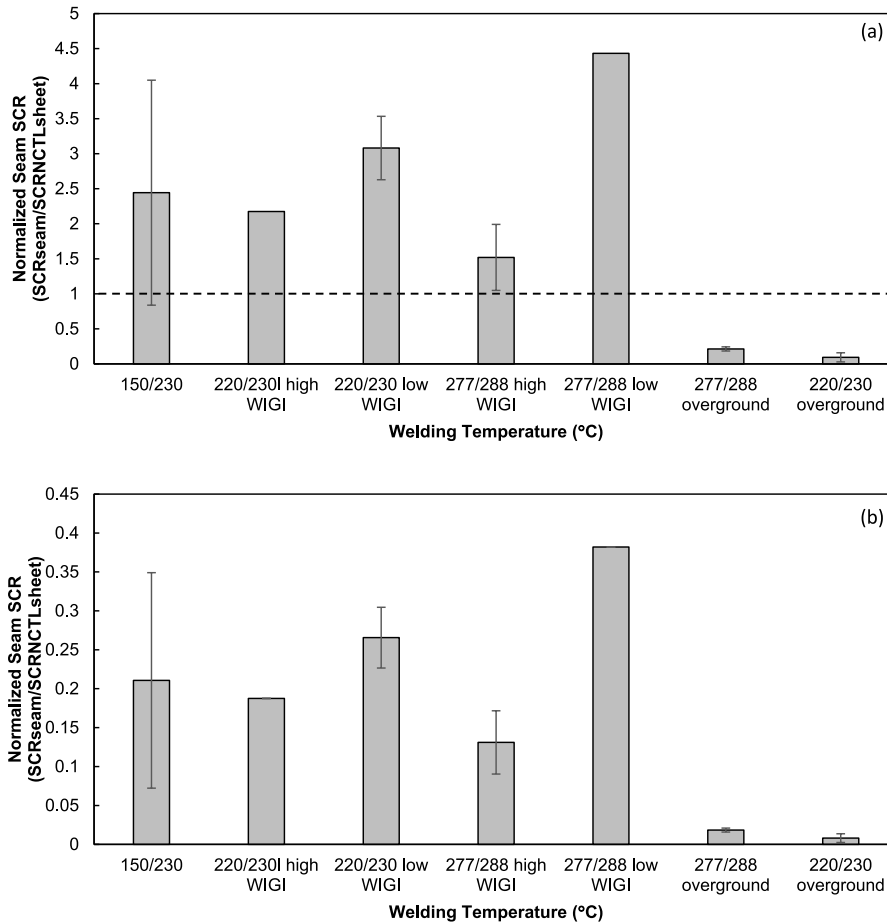


Fig. 15. Variation in normalized unnotched seam SCR for MwA-15 to ((a) notched sheet; (b) unnotched sheet). Error bars for individual parameter combinations represent max and min values for three replicates.

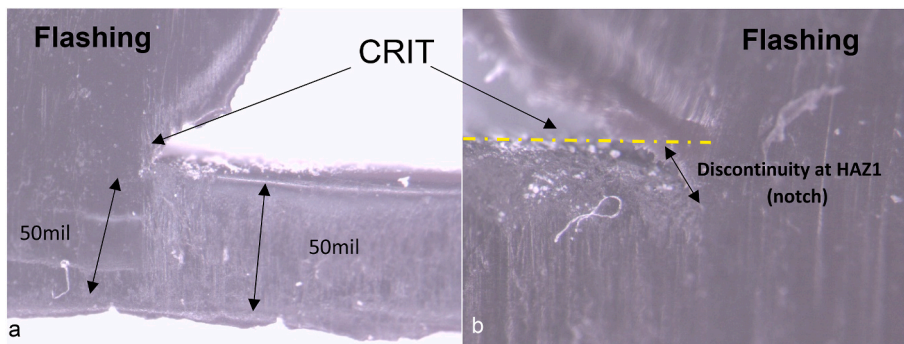


Fig. 16. Microscope photographic showing Craze which becomes stress crack adjacent to the flashing.

welding. However, operator-induced irregularities resulting in high WIGI ($\mu < 0.022$ or $\mu > 0.042$, see Fig. 2) could reduce the SCR by a factor of 3 or more, indicating the more attention should be paid to the geometric irregularities (WIGI) of extrusion welds and welds with high WIGI should not be acceptable even if pass the standard tests. The HAZ immediately adjacent to flashing is the critical location for stress cracking. Any stress concentration induced by surface defects at this location will further reduce the SCR and should be avoided. Lastly, welds exhibiting surface overground adjacent to CRIT resulted in a 97% reduction in unnotched SCR compared to normal ground welds. Therefore, CQA should routinely identify and reject (a) high WIGI extrusion welds with notable scratches/defects in the HAZ adjacent to

flashing, and (b) welds exhibiting overground surfaces adjacent to flashing. Trial welds should be conducted to check welds at the start of a shift, but this does not replace the need for careful visual inspection of all extrusion welds by CQC/CQA personnel.

4. Conclusions

Extrusion welds prepared by an experienced welding technician on a geomembrane with a sheet temperature of 37 °C for a combination of preheat temperatures (150, 220, and 277 °C), and barrel temperatures (230 °C, and 288 °C) were examined with a focus on SCR of extrusion welds. Consistent with the recommendation of [Francey and Rowe](#)

Table 6

List parameter combinations examined for MwA-15 fusion and extrusion weld and their corresponding average unnotched SCR failure times.

Material	Notch	Type	Sheet temperature at the time of welding (°C)		Preheat Temp (°C)	Barrel Temp (°C)	Wedge Temp (°C)	Welding Speed (m/min)	Average Failure Time (hours)	Normalized average failure time	Maximum (hours)	Minimum (hours)
MwA-15	Notched	virgin sheet	–	SAW	N/A	N/A			1012		1097	896
		Unnotched virgin sheet			N/A	N/A			11740	1	16963	8275
	Weld	Weld	37	Extrusion	150	230			2473	0.21	3622	1324
					220	230			2889	0.25	3384	2201
					220 ^a	230 ^a			95 ^a	0.01 ^a	141 ^a	48 ^a
					277 ^a	288 ^a			216 ^a	0.02 ^a	226 ^a	183 ^a
					277	288			2520	0.21	4484	1061
					65	Fusion ^b	460	1.8	2660	0.23	3050	2060
		400	3	3010	0.26		3990	2100				
		352	2.5	1710	0.15		2500	1200				
	21	Weld	460	1.8	1990	0.17	2450	1120				
			400	3	2860	0.24	3790	1810				
352			2.5	3970	0.34	4590	2930					

^a Overground extrusion weld.^b Data from Francey and Rowe (2022).

(2022) that unnotched specimens should be used to evaluate the SCR of the fusion welds, unnotched specimens were used to evaluate the extrusion welds examined in this paper. The paper has paid particular attention to the role of weld-induced geometric irregularity (WIGI) of extrusion welds. For the extrusion welds and geomembrane examined in this paper, the following conclusions were reached.

1. The virgin Std-OIT was highest in the weld area (i.e., bead and flashing). This is attributed to the high concentration of antioxidants in the welding rod.
2. The initial Std-OIT_{welding rod} of the welding rod was more than twice that of the sheet (Std-OIT_{welding rod} > 2 x Std-OIT_{sheet}) and this difference was needed to ensure that the final extruded weld bead had an initial Std-OIT_{bead} ~ 1.1 x Std-OIT_{sheet} after welding. It may be inferred that if the welding rod had the same initial Std-OIT_o as the sheet, the weld would have only about half that of the sheet after welding.
3. There was no statistically significant difference between average fusion and extrusion “normal ground” welds in terms of unnotched stress crack resistance. Thus, an extrusion weld is not necessarily worse than a fusion weld, but the extrusion weld was far more susceptible to significant operator induced variability that can reduce the SCR of the weld to less than 1% of the best extrusion weld.
4. Good extrusion welds with “low WIGI” had an unnotched SCR of 52% of that of the unnotched sheet.
5. Extrusion welds with high WIGI had a SCR of ≈9% of the unnotched sheet and about of third of that good extrusion weld.
6. Overgrinding of the surface reduced the unnotched weld SCR to between 1 and 6% of that of generally good extrusion welds and between 0.8 and 4% of the best extrusion weld.

It is acknowledged that this study only examined extrusion welds for one 1.5 mm smooth geomembrane. However, the results strongly suggest that CQA should routinely identify and reject high WIGI extrusion welds, extrusion welds with notable scratches/defects in the HAZ adjacent to flashing, and welds exhibiting overground surfaces adjacent to flashing. The effect of welding parameters, high WIGI, and overgrind on the reduction of SCR with ageing requires further investigation. Further studies are also needed to compare the long-term behaviour of SCR between extrusion and fusion welds.

CRediT authorship contribution statement

R. Kerry Rowe: Conceptualization, Formal analysis, Funding acquisition, Investigation, Methodology, Project administration, Resources, Supervision, Validation. **M. Mouhamed Ali:** Data curation, Formal analysis, Investigation, Methodology, Validation, Writing – original draft.

Data availability

Data will be made available on request.

Acknowledgments

The research presented in this paper was supported by the Natural Sciences and Engineering Council of Canada (NSERC Discovery Grant RGPIN/03928-2022) and a Geosynthetic Institute (GSI) fellowship grant. The equipment used was provided by funding from the Canada Foundation for Innovation (CFI) and the Government Ontario’s Ministry of Research and Innovation.

References

- Abdelaal, F.B., Rowe, R.K., Brachman, R.W.I., 2014. Brittle rupture of an aged HPDE geomembrane at local gravel indentations under simulated field conditions. *Geosynth. Int.* 21, 1–23.
- ASTM, 2013. D1238 Standard Test Method for Melt Flow Rates of Thermoplastics by Extrusion Plastometer. American Society for Testing and Materials, West Conshohocken, Pennsylvania, USA.
- ASTM, 2019. D3895 Standard Test Method for Oxidative Induction Time of Polyolefins by Differential Scanning Calorimetry. American Society for Testing and Materials, West Conshohocken, Pennsylvania, USA.
- ASTM, 2020. D5397 Standard Test Method for Evaluation of Stress Crack Resistance of Polyolefin Geomembranes Using Notched Constant Tensile Load Test. ASTM International, West Conshohocken, PA, USA.
- Clinton, M., Rowe, R.K., 2023. Antioxidant-stabilizer depletion of 4 HDPE geomembranes with high HP-OIT in MSW leachate. *Geosynth. Int.* Accepted 19/7/20243, GEIN-2023-041).
- Darilek, G.T., Laine, D.L., 2001. Costs and Benefits of geomembrane liner Installation CQA. In: *Proceedings of the Geosynthetics 2001 Conference*, Portland, OR, USA.
- DVS 2225-1, 2016. Welding of Lining Membranes Made of polyethylene (PE) for Protection of Groundwater. German Welding Society, Dusseldorf, Germany.
- Emcon Associates, 1994. Northridge Earthquake Seismic Evaluation, Chiquita Canyon Landfill, April.
- Ewais, A.M.R., Rowe, R.K., Brachman, R.W.I., Arnepalli, D.N., 2014. Service life of a high-density polyethylene geomembrane under simulated landfill conditions at 85 degrees C. *J Geotech Geoenviron* 140.
- Francey, W., Rowe, R.K., 2022. Stress crack resistance of unaged high-density polyethylene geomembrane fusion seams. *Geosynth. Int.*

- Gilson-Beck, A., Giroud, J.P., 2022. A quantification of the short-term reliability of HDPE geomembrane seaming methods. *Geosynth. Int.*
- Giroud, J.P., 2005. Quantification of geosynthetic behaviour. *Geosynth. Int.* 12, 2–27.
- Giroud, J.P., Tisseau, B., Soderman, K., Beech, J., 1995. Analysis of strain concentration next to geomembrane seams. *Geosynth. Int.* 2 (No. 6), 1049–1097.
- GRI-GM13, 2019. Standard Specification for Test Methods, Test Properties, and Testing Frequency for High Density Polyethylene (HDPE) Smooth and Textured Geomembranes. Geosynthetic Research Institute, Pennsylvania, USA.
- GRI-GM5(c), Seam Constant Tensile Load (SCTL) Test for Polyolefin Geomembrane Seams, Geosynthetic Research Institute, Drexel, PA, USA.
- Halse, Y.H., Koerner, R.M., Lord, A.E., 1990. Stress cracking Morphology of polyethylene (Pe) geomembrane seams. *Geosynthetics : Microstructure and Performance* 1076, 78–89.
- Hsuan, Y.G., 2000. Data base of field incidents used to establish HDPE geomembrane stress crack resistance specifications. *Geotext. Geomembranes* 18, 1–22.
- Hsuan, Y.G., Koerner, R.M., 1998. Antioxidant depletion lifetime in high density polyethylene geomembranes. *J Geotech Geoenviron* 124, 532–541.
- Kavazanjian, E., Arab, M., Matasovic, N., 2013. Performance of two geosynthetic-lined landfills in the Northridge earthquake. Proceedings of the 7th International Conference on Case Histories in Geotechnical Engineering. Missouri University of Science and Technology, Rolla, MO, USA.
- Kavazanjian, E., Andresen, J., Gutierrez, A., 2017. Experimental evaluation of HDPE geomembrane seam strain concentrations. *Geosynth. Int.* 24, 333–342.
- Marta, A., Armstrong, C., 2020. Brittle Stress Cracking of HDPE Geomembrane Caused by Localized Over-heating of Fusion Wedge Welds. *GeoAmericas, Brazil*, 2020.
- Mollard, S.J., Jefford, C.E., Staff, M.G., Browning, G.R.J., 1996. Geomembrane landfill liners in the real world. Geological Society, London, Engineering Geology Special Publications 11, 165–170, 1996.
- Morsy, M.S., Rowe, R.K., 2020. Effect of texturing on the longevity of high-density polyethylene (HDPE) geomembranes in municipal solid waste landfills. *Can. Geotech. J.* 57, 61–72.
- Morsy, M.S., Rowe, R.K., Abdelaal, F.B., 2021. Longevity of 12 geomembranes in chlorinated water. *Can. Geotech. J.* 58, 479–495.
- Peggs, I.D., Carlson, D.S., 1990a. Brittle-Fracture in Polyethylene Geomembranes. *Geosynthetics : Microstructure and Performance* 1076, 57–77.
- Peggs, I.D., Carlson, D.S., 1990b. The effects of seaming on the Durability of adjacent polyethylene geomembranes. *Am Soc Test Mater* 1081, 132–142.
- Peggs, I.D., Gassner, F., Scheirs, J., Tan, D., Noval Arango, A.M., Burkard, B., 2014. Is There a Resurgence of Stress Cracking in HDPE Geomembranes, 10th International Conference on Geosynthetics. ICG 2014.
- Rollin, A.L., Marcotte, M., Jacqueline, T., Chaput, L., 1999. Leak location in exposed geomembrane liners using an electrical leak detection technique. In: Proceedings of Geosynthetic 99 Industrial Fabrics Association International.
- Rowe, R.K., 1988. Contaminant migration through groundwater: the role of modelling in the design of barriers. *Can. Geotech. J.* 25 (4), 778–798 [Canadian Geotechnical Colloquium for 1987].
- Rowe, R.K., 1991. Contaminant impact assessment and the contaminating lifespan of landfills. *Can. J. Civ. Eng.* 18 (2), 244–253.
- Rowe, R.K., Islam, M.Z., 2009. Impact of landfill liner time-temperature history on the service life of HDPE geomembranes. *Waste Manag.* 29, 2689–2699.
- Rowe, R.K., Rimal, S., Sangam, H.P., 2009. Ageing of HDPE geomembrane exposed to air, water and leachate at different temperatures. *Geotext. Geomembr.* 27 (2), 131–151.
- Rowe, R.K., Shoaib, M., 2017. Long-term performance of high-density polyethylene (HDPE) geomembrane seams in municipal solid waste (MSW) leachate. *Can. Geotech. J.* 54, 1623–1636.
- Rowe, R.K., Shoaib, M., 2018. Durability of HDPE geomembrane seams immersed in brine for three Years. *J Geotech Geoenviron* 144.
- Rowe, R.K., Quigley, R.M., Brachman, R.W.I., Booker, J.R., 2004. Barrier Systems for Waste Disposal Facilities, 2nd. Spon Press, New York, USA.
- Rowe, R.K., Abdelaal, F.B., Zafari, M., Morsy, M.S., Priyanto, D.G., 2020. An approach to geomembrane selection for challenging design requirements. *Can. Geotech. J.* 57 (10), 1550–1565. <https://doi.org/10.1139/cgj-2019-0572>.
- Scheirs, J., 2009. A Guide to Polymeric Geomembranes: A Practical Approach. John Wiley & Sons, West Sussex, UK.
- Seeger, Muller, 2003. Theoretical approach to designing protection: selecting a geomembrane strain criterion. In: Dixon, N. (Ed.), Proceedings of the 1st IGS UK Chapter National Geosynthetics Symposium Held at the Nottingham Trent University on 17 June 2003. Thomas Telford Publishing, London, UK, pp. 137–151.
- Sieracke, M., Peggs, I.D., 2013. Thermal seaming of polyethylene geomembranes. In: Proceedings of the Geosynthetics 2013 Conference, Long Beach, CA (April 2013).
- Tian, K., Benson, C.H., Tinjum, J.M., Edil, T.B., 2017. Antioxidant depletion and service life prediction for HDPE geomembranes exposed to low-level radioactive waste leachate. *J. Geotech. Geoenviron. Eng.* 143 (6), 04017011 [https://doi.org/10.1061/\(ASCE\)GT.1943-5606.0001643](https://doi.org/10.1061/(ASCE)GT.1943-5606.0001643).
- Tian, K., Benson, C.H., Yang, Y.-M., Tinjum, J.M., 2018. Radiation dose and antioxidant depletion in a HDPE geomembrane. *Geotext. Geomembranes* 46 (4), 426–435. <https://doi.org/10.1016/j.geotextmem.2018.03.003>.
- Toepfer, G.W., 2015. Extrusion seams – the good, the bad, and the ugly. In: Geosynthetics Conference Proceedings, Portland, OR, USA, pp. 108–117.
- Touze-Foltz, N., Lupo, J., Barroso, M., 2008. Geoenvironmental applications of geosynthetics, Keynote Lecture. In: Proc Eurogeo 4, 98 the 4th European Conference on Geosynthetics, Edinburgh, Scotland, UK.
- Zafari, M., Abdelaal, F.B., Rowe, R.K., 2023a. Degradation behaviour of two multi-layered textured white HDPE geomembranes and their smooth edges. *ASCE J Geotech. Geoenviron* 149 (5). https://doi.org/10.1061/JGGEFK.GTENG-11101_04023020_1-0402302015.
- Zafari, M., Abdelaal, F.B., Rowe, R.K., 2023b. Long-term performance of conductive-backed multi-layered HDPE geomembranes. *Geotext. Geomembr.* 51 (4), 137–155.
- Zafari, M., Rowe, R.K., Abdelaal, F.B., 2023c. Longevity of multi-layered textured HDPE geomembranes in low-level waste applications. *Can. Geotech. J.* 57/2023; cgj-2023-0039.
- Zhang, L., Bouazza, A., Rowe, R.K., Scheirs, J., 2017. Effect of welding parameters on properties of HDPE geomembrane seams. *Geosynth. Int.* 24, 408–418.